

Polymer Mixed Matrix Membrane with Biosynthesized Zinc Oxide/Silver Oxide Additive for Antibacterial Performance

Faiz Hafeez Azhar¹, Amer Zakwan Zulkiplie¹, Zawati Harun^{1*}, Raja Adibah Raja Ahmad¹, Nurul Izwanie Rasli²

¹ Advanced Manufacturing and Materials Centre (AMMC), Faculty of Mechanical and Manufacturing Engineering, Universiti Tun Hussein Onn Malaysia (UTHM), 86400, Parit Raja, Batu Pahat, Johor, MALAYSIA

² Faculty of Applied Sciences and Technology, Universiti Tun Hussein Onn Malaysia (UTHM), Pagoh Education Hub, 84600, Muar, Johor, MALAYSIA

*Corresponding Author: zawati@uthm.edu.my
DOI: <https://doi.org/10.30880/emait.2025.06.01.005>

Article Info

Received: 13 April 2025
Accepted: 1 May 2025
Available online: 10 June 2025

Keywords

Zinc oxide, silver oxide, mixed matrix membrane, antibacterial

Abstract

Membrane technology has emerged as one of the most effective approaches for water purification, utilizing pore separation to achieve filtration without the complexities and high energy consumption associated with the traditional methods. Recent advancements have focused on modifying polymeric membranes, particularly polysulfone (PSf), by incorporating inorganic additives such as zinc oxide (ZnO) and silver oxide (AgO) nanoparticles. Thus, in this study, polymer MMMs were fabricated by incorporating biosynthesized ZnO/AgO synthesized from tea leaf extract as a reducing agent with the aim of enhancing membrane characteristics and antibacterial properties. The results showed that the antibacterial properties were enhanced by the addition of additives, particularly at higher concentrations of ZnO along with the presence of AgO. Other characteristics such as morphology, surface roughness, porosity, and hydrophilicity also produced the same increasing trend. These results proved that the addition of additives was able to enhance MMMs capabilities especially in terms of antibacterial properties.

1. Introduction

For centuries, diverse techniques have been employed to clean contaminated water, including filtration, distillation, and reverse osmosis [1]. Among these, membrane technology is one of the most effective approaches for water purification. This method utilizes pore separation without complex systems, high energy consumption, or increased expenses. Currently, researchers and technologists are intensively investigating, exploring, and advancing this technology. One area of focus is the modification of membranes using additives such as zinc oxide (ZnO) and silver oxide (AgO) nanoparticles to enhance the performance of polymeric membranes, particularly polysulfone (PSf) membranes. These inorganic additives are incorporated to boost various membrane properties, including the flow rate, solute rejection, and resistance to fouling [2].

ZnO nanoparticles are renowned for their antibacterial qualities and capacity to boost membrane hydrophilicity. When integrated into PSf membranes, they can enhance water flow and diminish fouling by increasing the effective surface area and introducing additional functional groups. Similarly, AgO nanoparticles exhibit antibacterial properties and have been demonstrated to improve the mechanical durability and hydrophilicity of PSf membranes [3]. The inclusion of AgO can substantially reduce membrane fouling, making it

suitable for water purification applications. The incorporation of these additives into the PSf matrix can be achieved by introducing them during the preparation of the polymer solution or in the coagulation bath. This adaptability enables the customization of the membrane characteristics to suit specific application requirements.

As for synthesizing of ZnO and AgO, tea, a globally popular beverage, contains phytochemicals, such as flavonoids, polyphenols, terpenoids, and amino acids that can efficiently reduce metal ions to nanoparticles. Studies show that Green and oolong tea extracts are effective in synthesizing AgO and possibly ZnO. This green synthesis method using tea extracts avoids toxic chemicals, reduces the environmental impact, and enhances safety. The reduction mechanism involves electron donation from the phytochemicals in the tea to the metal ions in solution. For example, mixing silver nitrate (AgNO_3) with tea extract results in a color change, indicating the formation of AgO. This method is efficient and produces nanoparticles with unique properties such as antimicrobial activity.

In the present work, polymer mixed matrix membranes (MMMs) incorporated with biosynthesized additives of AgO/ZnO were investigated to evaluate the characteristics of MMMs along with their antibacterial properties. The antibacterial properties of MMMs are crucial for enhancing their performance in various applications, particularly water treatment and filtration. The use of nanoparticles such as ZnO and AgO in MMMs has been shown to significantly improve antibacterial activity. These nanoparticles release ions that can disrupt bacterial cell membranes or inhibit their metabolic functions, leading to effective bacterial reduction. In addition, the addition of antibacterial agents not only enhanced the antibacterial properties but also improved other membrane characteristics, such as morphology, porosity, and permeability. This dual enhancement makes MMMs more suitable for demanding applications where both filtration efficiency and microbial control are required.

2. Materials and Methods

2.1 Biosynthesis of ZnO-AgO Additives

The synthesis process was performed according to Yusoff et al. with some modifications [4]. Dried tea leaves were purchased from a nearby market at Parit Raja, Batu Pahat, Johor. Dried tea leaves (50 g) were blended with 250 ml of deionized water for 6 h before being filtered and stored in a refrigerator. Then, powders of zinc nitrate hexahydrate ($\text{Zn}(\text{NO}_3)_2$, Sigma Aldrich, 99%) and silver nitrate ($\text{Ag}(\text{NO}_3)_3$, EMPARTA®) were utilized in the aqueous solution by using 5.94 g of $\text{Zn}(\text{NO}_3)_2$ and 3.49 g of $\text{Ag}(\text{NO}_3)_3$, respectively. Both beakers were mixed with 200 ml of deionized water and stirred for 30 min. Each solution was then mixed with the tea extract as reduction agent according to the design parameters shown in Table 1. The mixed solutions were stirred for 6 h at a hot-plate temperature of 60°C. The samples were then dried at 80°C for 24 h to discharge the ZnO-AgO nanoparticles. The samples were ground with mortar to get a fine dark brown powder.

Table 1 Parameter ratio for biosynthesized ZnO-AgO additives

Samples	Tea (ml)	$\text{Zn}(\text{NO}_3)_2$ (ml)	AgNO_3 (ml)
20-ZnO/AgO	20	20	10
40-ZnO/AgO	20	40	10
60-ZnO/AgO	20	60	10

2.2 MMM Fabrications

Referring to previous studies, the process of MMM fabrication was performed by drying 15 g of PSf pellets (Udel P-1700) at 60°C overnight before being dissolved in 85 g of N-methyl-2-pyrrolidone (NMP, EMPLURA®) as a solvent containing 1 g of designated ((20)ZnO-AgO, (40)ZnO-AgO), and (60)ZnO-AgO) additives for 4 h at 500 rpm and 60°C with stirring [5]. Polyethylene glycol 400 MW (PEG-400, R&M Chemical®) as a pore-forming agent was added to the polymer dope solutions. After an hour, the doped polymer was placed in an electrostatic machine for 0.5 h and left for 15 min to release the bubbles. A flat-sheet MMM was prepared by casting the polymer dope onto a glass plate with a thickness of 100-120 µm. The phase inversion process was performed by separately immersing each MMM into a coagulation bath containing distilled water. After the membranes were detached, the membranes were dried for 24 h.

2.3 Characterization and Performance Test of Additives and MMMs

X-ray diffraction (XRD) was employed to analyze the structural characteristics of ZnO-AgO additives. The analysis was conducted using a Bruker® D8 Advanced instrument with the following parameters: 45 kV operating voltage, 40 mA current, Cu K α monochromatic radiation ($\lambda = 1.5406 \text{ \AA}$), 2θ range of 10–90°, and a step increment rate of

0.05°/min. The resulting XRD data was subsequently evaluated using EVA software and cross-referenced with the Joint Committee on Powder Diffraction Standards (JCPDS) database for comparison.

The cross-sectional morphology of the MMMs was examined using a Hitachi U1510 scanning electron microscope (SEM) at 15 kV. To preserve the structural integrity of the membranes, all samples were prepared by breaking the membrane film in liquid nitrogen. Subsequently, the membranes were coated with gold before being mounted on the SEM platform for analysis. Attenuated total reflection-Fourier transform infrared spectroscopy (ATR-FTIR, PerkinElmer®) was utilized to analyze the chemical interactions of each MMM. The examination was conducted within the range of 4000 cm⁻¹ to 600 cm⁻¹ wavenumbers. The topography and surface roughness of each MMM were evaluated using atomic force microscopy (AFM, XE-Series Park Systems®). Measurements were taken on specific 1 μm² areas of the MMMs. To obtain average values of mean roughness (Ra), each membrane underwent three separate scans. For porosity, the MMMs were set up by cutting them into 2 cm² pieces. The MMMs were then immersed in distilled water for 24 h and scaled in the wet state (W_w). Subsequently, the MMMs were dried in an oven at 60°C for 24 h before being scaled again for the dry state, W_d . The test was performed thrice, and the average was used to obtain an accurate porosity value. The value was calculated using the following Equation (1), where ρ_w (g/cm³) denotes the density of pure water at room temperature and V (cm³) represents the volume of membrane in wet state:

$$\text{Porosity, } \varepsilon = (W_w - W_d) / (\rho_w - V) \quad (1)$$

Escherichia coli (E. coli) was chosen for antibacterial testing, as this microorganism is typically found in the natural organic matter (NOM) of authentic wastewater. A circular section, measuring 50.0 mm in diameter, was punched from each MMM and introduced into a culture medium. The samples were then incubated at 37°C, and the bacterial reaction was examined after a 24 h period. Meanwhile, the pure water flux (PWF) test was utilized to assess the performance of MMMs. Each MMM was carefully cut into a circular shape with a surface area of 2.8 cm² and affixed to a membrane cell. The PWF test proceeded at a specific pressure of 5 bar until the distilled water flow reached a steady state. Subsequently, PWF values were determined at 2 bar pressure, recorded at 10 min intervals, and calculated using Equation (2), where, Q represents the volume of permeate water, A (m²) denotes the effective membrane surface area and Δt (h) indicates the permeation time:

$$\text{Pure water flux, } J = (Q) / (A \times \Delta t) \quad (2)$$

3. Result and Discussion

3.1 Structural and Morphology Properties of Synthesized ZnO-AgO

As shown in Fig. 1 (a), 60-ZnO/AgO showed a higher intensity in the XRD spectrum than the 40-ZnO/AgO and 20-ZnO/AgO samples, indicating a more crystalline structure or a greater amount of crystalline material present in the 60-ZnO/AgO formulation. Three significant peaks are observed at 38.6°, 32.3°, and 44.3°, corresponding to Ag and Zn. Smaller peaks are observed at 18.9° and 46.5°, corresponding to ZnO and AgO, respectively. These patterns are similar to those reported by Arora et al. and Jeung et al. [6,7]. However, synthesis using tea extract as a reducing agent for silver nitrate and zinc nitrate faced challenges, as indicated by the XRD results. Although the expected products were AgO and ZnO, these oxides were only present at smaller peaks, suggesting minimal formation. In contrast, higher-intensity peaks for metallic Ag and Zn were observed, indicating that the reduction process favored the formation of metals over oxides. This suggests that the synthesis conditions and effectiveness of the tea extract as a reducing agent were suboptimal. Plant extracts may not fully convert metal ions into oxides; instead, they often reduce metal salts to their elemental forms, resulting in metallic nanoparticles (NPs) rather than oxides [8]. Parameters such as the temperature, pH, and reactant concentration significantly influence the synthesis process; if not optimized, they can favor metal formation. For instance, higher temperatures might accelerate reduction, leading to more metallic NPs formation [9].

Although the synthesized powder exhibits lower intensity peaks for AgO and ZnO, it may still demonstrate enhanced antibacterial capabilities due to the combined effects of Ag and ZnO and their individual antimicrobial mechanisms. The synergy between Ag NPs, known for their potent antibacterial properties, and ZnO, which generates reactive oxygen species (ROS), can boost the overall antimicrobial effectiveness of the nanocomposite, even when the oxide forms are present in smaller quantities [10]. Furthermore, ZnO nanoparticles show considerable antibacterial activity because of their diminutive size and large surface-to-volume ratio, enabling efficient interaction with bacterial cells. The inclusion of AgO can amplify this effect by compromising bacterial membranes and causing oxidative stress, ultimately resulting in cell death. Consequently, despite the lower oxide peaks, their presence can still contribute significantly to the overall antibacterial action of the material especially as additive for MMMs. [11].

As shown in the SEM images in Fig. 1(b), (c), and (d), all samples were distributed closely without any particular shape, leading to agglomeration. Agglomeration can obscure individual particle boundaries, making it challenging to determine the true size of particles. When the particles cluster, the measured dimensions may represent agglomerates rather than individual NPs.

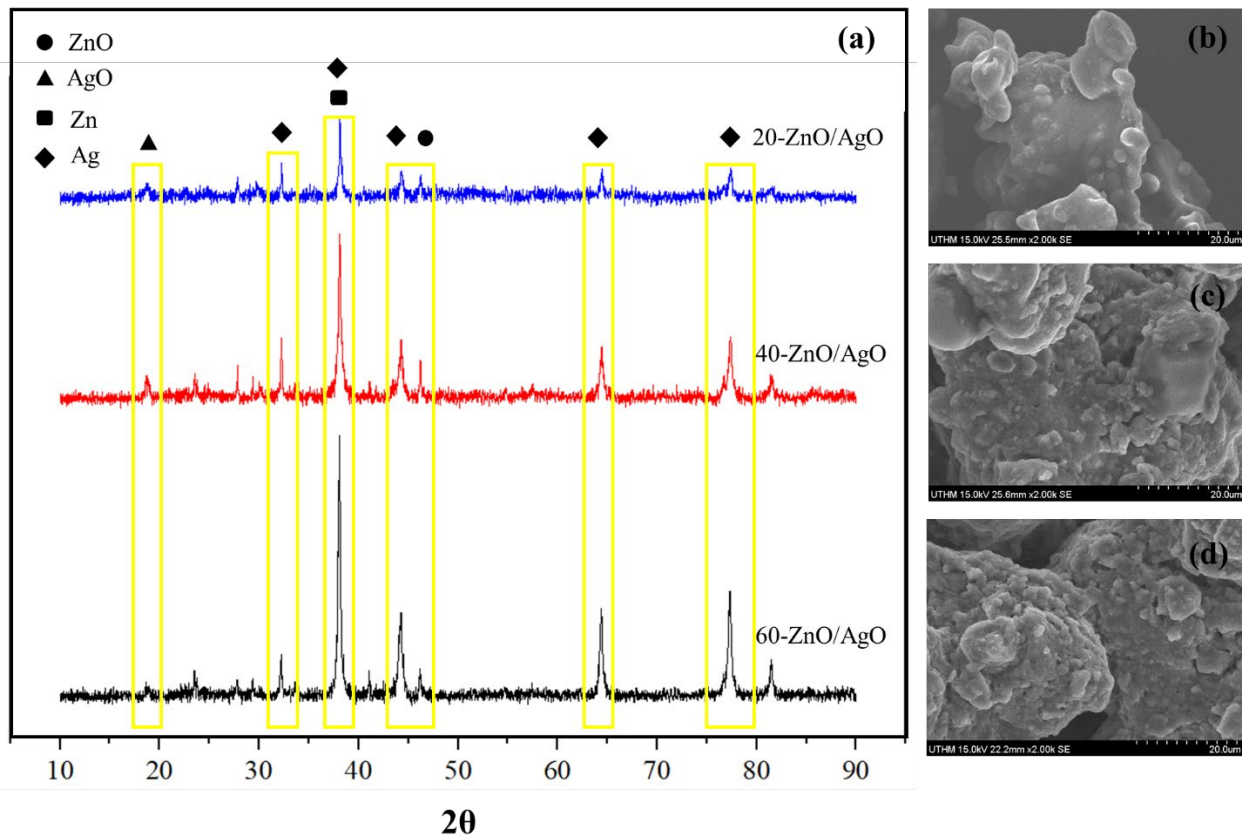


Fig. 1 (a) XRD of biosynthesis ZnO/AgO additives; SEM image of (b) 20-ZnO/Ag; (c) 40-ZnO/AgO; and (d) 60-ZnO/AgO

3.2 Morphology and Surface Roughness Analysis of MMMs

Fig. 2 (a), (b), and (c) show the cross-sectional images of the 20-ZnO/AgO MMM, 40-ZnO/AgO MMM, and 60-ZnO/AgO MMM, respectively. As the concentration of ZnO in the MMMs increased from 20 to 60 ml, a notable increase in the number of finger-like pores was observed in the top layer of the membranes. This trend suggests that a higher ZnO content enhances the formation of these specific pore structures during the phase-inversion process. An increase in the number of finger-like pores can improve the permeability of the membrane, allowing enhanced transport properties. This is particularly beneficial for applications that require efficient filtration or separation [12]. A similar phenomenon was observed in the bottom layer of the MMM, where the bottom layer exhibited greater porosity, which was attributed to the hydrophilic properties of the ZnO/AgO additive. The ability of these materials to attract water during the phase-inversion process facilitates the formation of more porous structures. During phase inversion, the interaction between the hydrophilic additive and water leads to solvent-induced phase separation, creating a more porous morphology. This increased porosity can enhance water permeability and improve the overall performance of the membrane in aqueous environments [13].

Fig. 2 (d), (e), and (f) represent the surface roughness obtained using AFM analysis. The analysis revealed that the average surface roughness of the MMMs increased with the ZnO concentration. This trend is corroborated by the topological images obtained from AFM, which visually demonstrate the changes in surface texture with increasing ZnO content. Higher surface roughness can enhance the effective surface area available for permeation, which is beneficial for filtration applications. This increased active area can improve the membrane's ability to facilitate mass transport and enhance overall permeability [14]. Although increased surface roughness can improve the permeation efficiency, it also raises concerns regarding fouling. Textured surfaces may trap foulants (such as organic matter, microorganisms, and particulate matter) more easily, potentially leading to reduced membrane performance over time. This fouling can result in increased resistance to flow and necessitate more frequent cleaning or replacement.

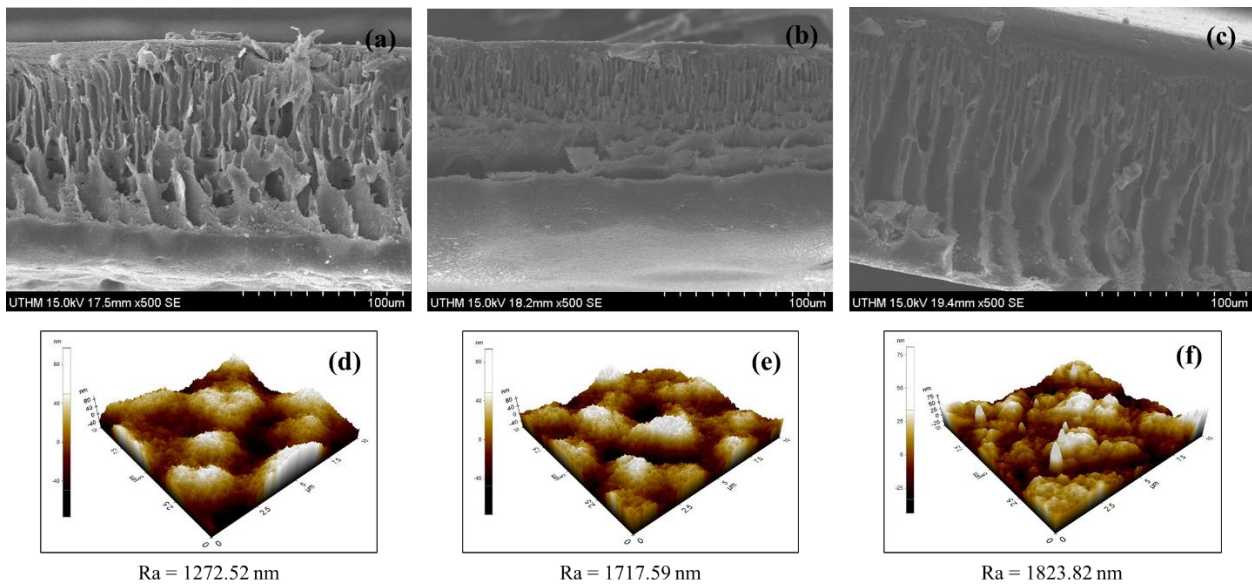


Fig. 2 Cross-sectional images of (a) 20-ZnO/AgO MMM; (b) 40-ZnO/AgO MMM; and (c) 60-ZnO/AgO MMM; and surface roughness of (d) 20-ZnO/AgO MMM; (e) 40-ZnO/AgO MMM; and (f) 60-ZnO/AgO MMM

3.3 Chemical Bonding and Porosity Analysis of ZnO-AgO MMMs

From the FTIR analysis shown in Fig. 3(a), the OH peak, which indicates the hydrophilicity of the membrane, produced a higher-intensity peak for 60-ZnO/AgO as an additive. Since the concentration of ZnO was only variable during powder synthesization, the impact of this properties might come from the increase of ZnO concentration, thus help boosting the mixed matrix membrane hydrophilicity propertites. The presence of ZnO/AgO, especially at higher concentrations, helps in the formation of hydroxyl groups on the surface, which contribute to the hydrophilic properties. It also might enhance water attraction due to the hydrophilic nature of ZnO nanoparticles, and thus might be able to improve water permeability, with some studies showing up to 300% improvement when optimized and more porous membrane structures that facilitate water transport align with the SEM analysis results [15].

As shown in Fig. 3 (b), when the concentration of zinc nitrate increased during synthesis, there was a corresponding increase in the membrane porosity, indicating that the zinc nitrate concentration strongly influences the formation of porous structures. This effect can be attributed to the oxidation process where zinc nitrate converts to zinc oxide, which serves as the primary factor in determining the membrane's porosity characteristics [16].

3.4 Permeation Performance of ZnO-AgO MMMs

Fig. 3(c) shows the PWF results for all the MMMs. The data showed a consistent trend, where permeation increased proportionally with higher ZnO concentrations in the membrane matrix. The membrane achieved its highest water flux of 206.65 L/m²h, which can be attributed to the incorporation of hydrophilic ZnO/AgO additives. This enhanced performance perfectly aligns with the other analytical results, particularly the intense OH peaks observed in the FTIR analysis and the increased membrane porosity measurements. The improvement in water flux can be attributed to several synergistic effects: the hydrophilic nature of the ZnO/AgO particles creates additional pathways for water transport, whereas surface hydroxyl groups enhance membrane wettability [17,18]. Furthermore, the combination of increased porosity and hydrophilicity creates optimal conditions for water permeation.

3.5 Antibacterial Properties of ZnO-AgO MMMs

The antibacterial performance of the MMMs was evaluated through inhibition tests against *E. coli* with samples incubated at 37 °C for 24 h. The results shown in Fig. 4 reveal significant antibacterial activity, particularly for the membrane containing 60-ZnO/AgO, which demonstrated the largest inhibition zone with a radius difference of 9.302 mm. This superior performance can be attributed to the even distribution of nanoparticles throughout the membrane matrix and the effective antibacterial properties of AgO synthesized using the tea leaf extract [19]. The enhanced antibacterial effectiveness appears to correlate directly with the increased concentration of ZnO in ZnO/AgO additives. This relationship is significant because ZnO possesses inherent antibacterial properties that

complement the antimicrobial action of AgO [20]. The combination of these two metal oxides creates a synergistic effect, resulting in more effective bacterial growth inhibition. Furthermore, although the XRD data indicate that metallic Ag may coexist with oxides, the primary antibacterial mechanism remains rooted in the designed ZnO/AgO additive. The low-intensity oxide peaks do not diminish the role of the oxide phases but highlight the complexity of the composite, where even trace oxides contribute significantly alongside metallic Ag. This aligns with studies showing that mixed oxide-metal systems (ZnO–Ag) outperform single-component systems [21,22]. Thus, the membrane’s antibacterial performance likely stems from the interplay of both phases, with the additive’s design driving the dominant mechanisms.

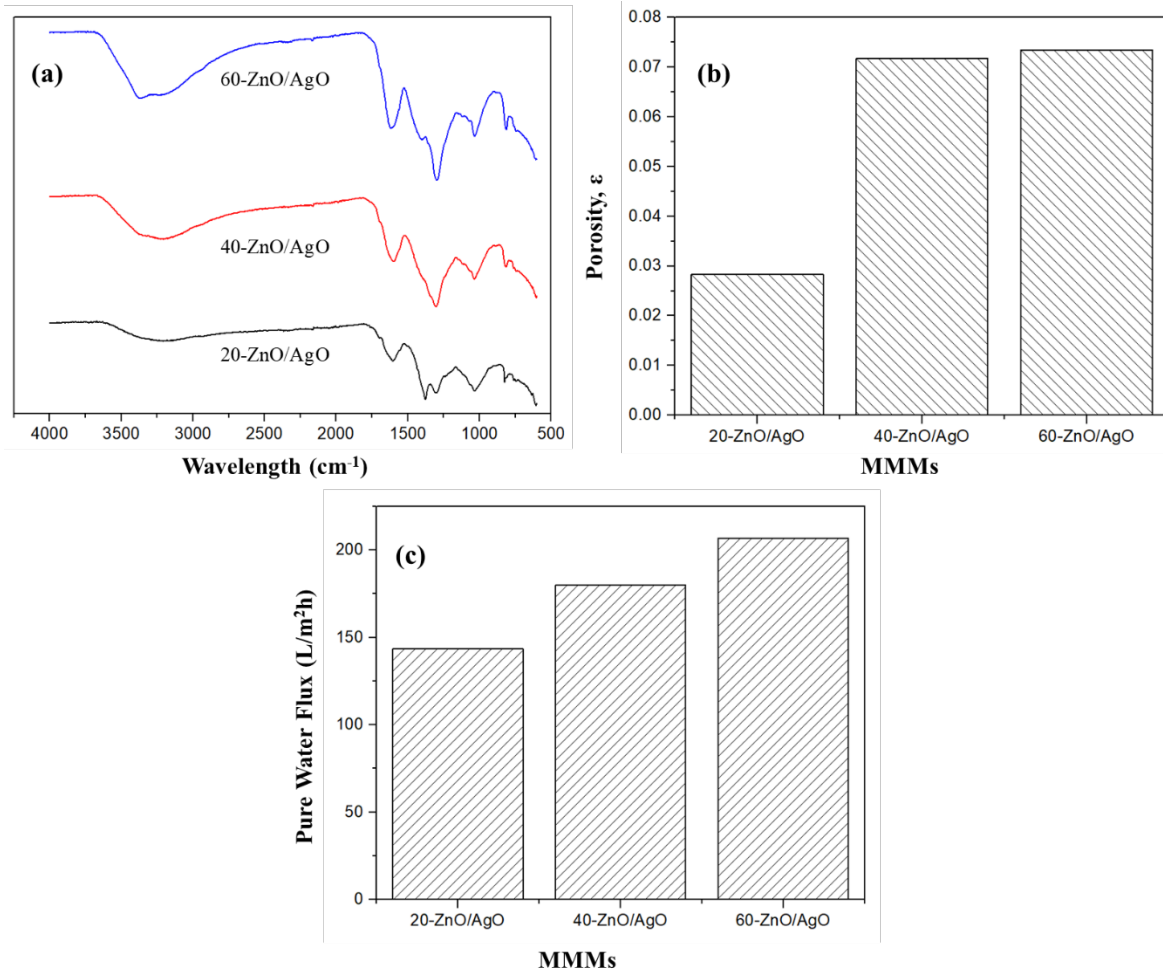


Fig. 3 (a) FTIR analysis; (b) Porosity analysis; and (c) Permeation performance of each MMMs

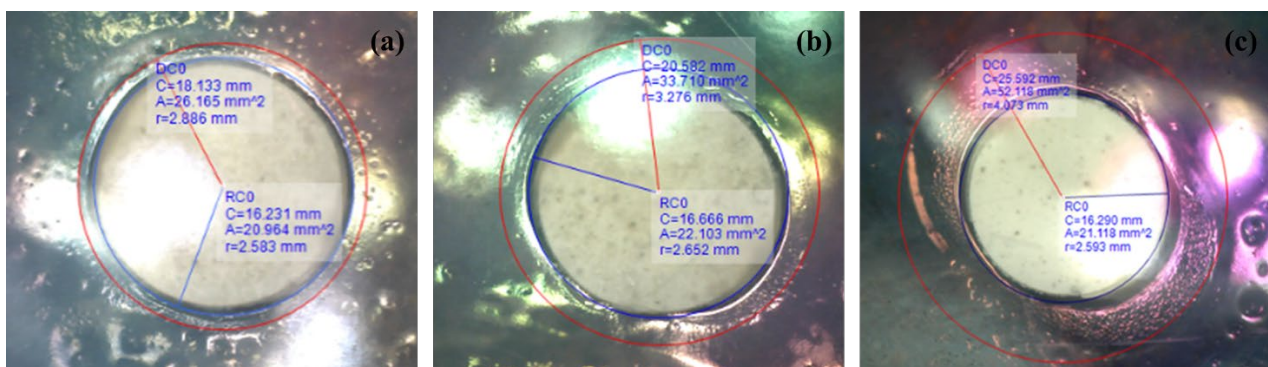


Fig. 4 Antibacterial properties of (a) 20-ZnO/AgO MMM; (b) 40-ZnO/AgO MMM; and (c) 60-ZnO/AgO MMM

4. Conclusion

To summarize, the incorporation of ZnO/AgO as an additive improved the characteristics and antibacterial properties of MMMs. Despite the synthesis process revealing stronger peaks for metallic Ag and Zn, suggesting a preference for metal formation over oxides, the material may still exhibit enhanced antimicrobial efficacy due to the synergistic effects of Ag and Zn and their respective antibacterial mechanisms. Nevertheless, the presence of smaller peaks indicating AgO and ZnO formation, albeit minimal, could contribute to the improved characterization and antibacterial qualities of both the powder and MMMs.

Acknowledgement

Recognition was given to the Advanced Manufacturing and Material Center (AMMC), Faculty of Mechanical and Manufacturing Engineering (FKMP), and Microelectronics and Nanotechnology-Shamsuddin Research Centre (MiNT-SRC) for providing the necessary facilities to conduct experimental work and laboratory testing.

Conflict of Interest

Authors declare that there is no conflict of interests regarding the publication of the paper.

Author Contribution

The authors confirm contribution to the paper as follows: **study conception and design:** Faiz Hafeez Azhar, Amer Zakwan Zulkiplie; **data collection:** Faiz Hafeez Azhar; **analysis and interpretation of results:** Faiz Hafeez Azhar, Amer Zakwan Zulkiplie, Raja Adibah Raja Ahmad; **draft manuscript preparation:** Faiz Hafeez Azhar, Zawati Harun. All authors reviewed the results and approved the final version of the manuscript.

References

- [1] Azhar, F. H., Harun, Z., Hussin, R., Ibrahim, S. A., Raja Ahmad, R. A., & Shohur, M. F. (2023). Methylene Blue Dye Wastewater Treatment Based On Tertiary Stage of Industrial Wastewater Treatment Process: A Review. *Emerging Advances in Integrated Technology*, 3(2), 37–51. <https://doi.org/10.30880/eamit.2022.03.02.004>
- [2] Sofian, M. S. M., Yunus, M. Z., Ahmad, A., Harun, Z., Akhair, S. H. M., Ahmad, R. A. R., Azhar, F. H., Rashid, A. Q. A., & Ismail, A. E. (2017). Effect of solvent concentration on performance of polysulfone membrane for filtration and separation. *IOP Conference Series: Materials Science and Engineering*, 226(1), 012171. <https://doi.org/10.1088/1757-899X/226/1/012171>
- [3] Rashid, A. Q. A., Harun, Z., Yunus, M. Z., Ahma, A., Ahmad, R. A. R., & Azhar, F. H. (2018). The coating effect of PANI/silver on performance of polysulfone membrane toward protein separation. *International Journal of Engineering, Transactions B: Applications*, 31(8), 1406–1412. <https://doi.org/10.5829/ije.2018.31.08b.32>
- [4] Yusoff, H. M., Idris, N. H., Hipul, N. F., Mahamad Yusoff, N. F., Nur, N. Z., & Irshad Ul Haq, B. (2020). Green synthesis of zinc oxide nanoparticles using black tea extract and its potential as anode material in sodium-ion batteries. *Malaysian Journal of Chemistry*, 22(2), 43–51.
- [5] Azhar, F. H., Harun, Z., Yunus, M. Z., Ibrahim, S. A., Hussin, R., Alias, S. S., Hubadillah, S. K., & Abdullahi, T. (2021). The effect of unique structural flower-like TiO₂ towards polysulfone mixed matrix membrane as efficient antifouling and antibacterial for humic acid removal. *Journal of Polymer Research*, 28(8), 1–17. <https://doi.org/10.1007/s10965-021-02644-5>
- [6] Arora, A. K., Devi, S., Jaswal, V. S., Singh, J., Kinger, M., & Gupta, V. . (2014). Synthesis and Characterization of ZnO Nanoparticles. *Oriental Journal of Chemistry*, 30(4), 1671–1679.
- [7] Jeung, D. G., Lee, M., Paek, S. M., & Oh, J. M. (2021). Controlled growth of silver oxide nanoparticles on the surface of citrate anion intercalated layered double hydroxide. *Nanomaterials*, 11(2), 1–16. <https://doi.org/10.3390/nano11020455>
- [8] Azad, A., Zafar, H., Raza, F., & Sulaiman, M. (2023). Factors Influencing the Green Synthesis of Metallic Nanoparticles Using Plant Extracts: A Comprehensive Review. *Pharmaceutical Fronts*, 05(03), e117–e131. <https://doi.org/10.1055/s-0043-1774289>
- [9] Drummer, S., Madzimbamuto, T., & Chowdhury, M. (2021). Green synthesis of transition-metal nanoparticles and their oxides: A review. *Materials*, 14(11). <https://doi.org/10.3390/ma14112700>
- [10] Fonseca, B. B., Silva, P. L. A. P. A., Silva, A. C. A., Dantas, N. O., De Paula, A. T., Olivieri, O. C. L., Beletti, M. E., Rossi, D. A., & Goulart, L. R. (2019). Nanocomposite of Ag-doped ZnO and AgO nanocrystals as a preventive measure to control biofilm formation in eggshell and salmonellaspp. Entry into eggs. *Frontiers in Microbiology*, 10(217), 1–10. <https://doi.org/10.3389/fmicb.2019.00217>
- [11] Gudkov, S. V., Burmistrov, D. E., Serov, D. A., Rebezov, M. B., Semenova, A. A., & Lisitsyn, A. B. (2021). A Mini Review of Antibacterial Properties of ZnO Nanoparticles. *Frontiers in Physics*, 9(March), 1–12.

- <https://doi.org/10.3389/fphy.2021.641481>
- [12] Southern, T. J. F., & Evans, R. C. (2021). Dual-template approach to hierarchically porous polymer membranes. *Materials Chemistry Frontiers*, 5(2), 783–791. <https://doi.org/10.1039/d0qm00610f>
- [13] Arahman, N., Mulyati, S., Fahrina, A., Muchtar, S., Yusuf, M., Takagi, R., Matsuyama, H., Nordin, N. A. H., & Bilad, M. R. (2019). Improving water permeability of hydrophilic PVDF membrane prepared via blending with organic and inorganic additives for humic acid separation. *Molecules*, 24(22), 4099 (1-13). <https://doi.org/10.3390/molecules24224099>
- [14] Miller, D. J., Dreyer, D. R., Bielawski, C. W., Paul, D. R., & Freeman, B. D. (2016). Surface Modification of Water Purification Membranes a Review. *Angewandte Chemie*, 17(129), 1–151. [https://doi.org/10.1016/0009-2509\(62\)87032-8](https://doi.org/10.1016/0009-2509(62)87032-8)
- [15] Adilah Rosnan, N., Haan, T. Y., & Mohammad, A. W. (2018). The effect of ZnO loading for the enhancement of PSF/ZnO-GO mixed matrix membrane performance. *Sains Malaysiana*, 47(9), 2035–2045. <https://doi.org/10.17576/jsm-2018-4709-11>
- [16] Berg, T. van den, & Ulbricht, M. (2020). Polymer nanocomposite ultrafiltration membranes: The influence of polymeric additive, dispersion quality and particle modification on the integration of zinc oxide nanoparticles into polyvinylidene difluoride membranes. *Membranes*, 10(9), 1–19. <https://doi.org/10.3390/membranes10090197>
- [17] Abdulkarim, A. A., Ahmad, A. L., Ismail, S., & Ooi, B. S. (2013). Preparation and characterization of polyethersulfone membrane containing zinc oxide nanoparticles and polyvinylpyrrolidone. *Jurnal Teknologi (Sciences and Engineering)*, 65(4), 13–16. <https://doi.org/10.11113/jt.v65.2320>
- [18] Zahid, A., Nawaz, H. H., Siddique, A., Ahmed, B., Razzaque, S., Liu, X., Razzaq, H., & Umar, M. (2024). Enabling improved PSF nanocomposite membrane for wastewater treatment with selective nanotubular morphology of PANI/ZnO. *Materials Advances*, 9471–9487. <https://doi.org/10.1039/d4ma00859f>
- [19] Mohanaparameswari, S., Balachandramohan, M., Sasikumar, P., Rajeevgandhi, C., Vimalan, M., Pugazhendhi, S., Ganesh Kumar, K., Albukhaty, S., Sulaiman, G. M., Abomughaid, M. M., & Abu-Alghayth, M. (2023). Investigation of structural properties and antibacterial activity of AgO nanoparticle extract from Solanum nigrum/Mentha leaf extracts by green synthesis method. *Green Processing and Synthesis*, 12(1), 1–17. <https://doi.org/10.1515/gps-2023-0080>
- [20] Saliani, M., Jalal, R., & Goharshadi, E. K. (2015). Effects of pH and temperature on antibacterial activity of zinc oxide nanofluid against Escherichia coli O157: H7 and staphylococcus aureus. *Jundishapur Journal of Microbiology*, 8(2), 1–6. <https://doi.org/10.5812/jjm.17115>
- [21] Pandey, M., Singh, M., Wasnik, K., Gupta, S., Patra, S., Gupta, P. S., Pareek, D., Chaitanya, N. S. N., Maity, S., Reddy, A. B. M., Tilak, R., & Paik, P. (2021). Targeted and Enhanced Antimicrobial Inhibition of Mesoporous ZnO-Ag₂O/Ag, ZnO-CuO, and ZnO-SnO₂ Composite Nanoparticles. *ACS Omega*, 6(47), 31615–31631. <https://doi.org/10.1021/acsomega.1c04139>
- [22] Azhar, F. H., Harun, Z., Yusof, K. N., Ibrahim, S. A., Hussin, R., Basri, H., Alias, S. S., & Hairom, N. H. H. (2025). Enhancement of Antifouling and Antibacterial Properties of Biosynthesis Silver Nanoparticles from Parkia speciosa (Stink Bean) Polysulfone Mixed Matrix Membrane. *Fibers and Polymers*, 1–16. <https://doi.org/10.1007/s12221-025-00925-0>